FINAL DRAFT: Performance Analysis of MICS-based RF Wireless Power Transfer System for Implantable Medical Devices

AHMAD N. ABDULFATTAH[1], (Student Member, IEEE), CHARALAMPOS C. TSIMENIDIS[1], (Senior Member, IEEE), BESSAM Z. AL-JEWAD[2], (Member, IEEE), AND ALEX YAKOVLEV[1], (Fellow Member, IEEE)

[1]School of Engineering, Newcastle University, Newcastle upon Tyne, NE1 7RU, U.K.
[2]Department of Communication and Computer Engineering, Cihan University, Erbil, Iraq

Corresponding author: Ahmad N. Abdulfattah (A.n.abdulfattah1@newcastle.ac.uk)

ABSTRACT In medical applications, implant devices are used to measure and remotely transmit the human biological signals to off-body devices. To date, providing the implantable medical devices (IMDs) with a constant and perpetual energy source remains an ongoing challenge. Accordingly, a far-field radio-frequency (RF) powering, represented by access point (AP), in conjunction with energy-harvesting capability is deployed in this paper for continuous powering of the IMDs. In this respect, theoretical analysis is used to establish safe powering conditions in order to comply with the safety limits established by the Federal Communications Commission. The feasibility of the wireless power transfer (WPT) to the IMDs is investigated by deriving analytical closed-form expressions for outage probability and average harvested energy, both of which are validated with Monte Carlo simulations. The findings of this study suggest not to exceed a distance of 0.5 m between the AP and the body surface, as the system performance has experienced high outage probability beyond this value, while the minimum allowable distance is 17 cm at a powering frequency of 403 MHz. It is also presented that the access point should be equipped with a minimum transmit power of 0.4 W in order to maintain an outage probability for the energy-harvesting to less than 10^{-1}.

INDEX TERMS Energy harvesting, implantable medical devices, outage probability, RF wireless power transfer.

I. INTRODUCTION

THE need for continuous monitoring of human biological signals has highlighted the vital role of implantable medical devices (IMDs) to improve the patient's health care [1]. Although the IMDs are low-energy consumption devices, supplying them with sufficient power for a long-lifetime is a main concern of many researchers. Conventionally, the limited lifespan batteries, or even the rechargeable ones, need a regular replacement and surgical intervention which in turn decreases patients comfort [2]. The new approach to solve this problem is to make the IMD energy self-sustaining by scavenging the energy from the ambient environments. Owing to that, energy-harvesting has emerged as a promising technology to supply the IMDs with permanent and sufficient power. Several methods of energy-harvesting currently exist for powering the IMDs. The human body offers abundant source of energy represented as breathing, body heat, body

motion or any other activity. For instance, biofuel cells implanted in a human body and operated by electrochemical reaction of the living organisms have been utilized by the authors in [3]–[5] as a source of energy to power the implanted devices. Kinetic/vibration energy is another source of energy that can be generated by human body activities. The piezoelectric is one of the kinetic energy types in which the mechanical energy is converted into electrical energy. A prototype of a shoe-mounted nonlinear piezoelectric energy harvester has been presented in [6] and has the capability of harvesting energy from human walking. The gradients in human temperature can also be exploited to produce thermoelectricity which can be converted to electrical energy to power energy-constrained devices like the IMDs [7]. Thermoelectric generator (TEG) has been used by the authors in [8]–[10] to produce the electrical energy where it is usually implanted very close to skin for the purpose of getting highest

A. N. Abdulfattah *et al.*: Performance Analysis of MICS-based RF Wireless Power Transfer System for Implantable Medical Devices

IEEE *Access*

temperature gradient. Other researchers implant a solar panel under the skin and exploited the sunlight and artificial light sources to power an IMD operated by subcutaneous solar energy-harvesting [11], [12]. According to the fact that all the aforementioned energy sources are usually climate or location dependent, the energy harvested from radio-frequency (RF) using wireless power transfer (WPT) system is a strong candidate among all the variety of energy sources to guarantee a perpetual energy source and continuous operation of the IMDs [13].

The use of WPT technology eliminates the risk of battery replacement and enables the implants to operate for indefinite period of time. Near-field (NF) WPT systems have been well studied and utilized by many researchers to charge and communicate with the bio-medical implants [14]–[16]. However, several constraints have been reported in such systems. For instance, in addition to the fact that the distance between the power supply and the IMD can not exceed few centimeters, an accurate alignment is required between the internal and external coils which, in some cases, is difficult to apply [17]. Another type of WPT technique which also commonly used to power the IMDs is the magnetic resonant coupling. This method is characterized by its high power transfer efficiency and has been used by [15] and [18] for powering ventricular assist device where a diameter of $22 \, \mathrm{mm}$ and $9.5 \, \mathrm{cm}$ of implantable wire coils are employed for power delivery. However, the frequency used in this method is very low which in turn limits the channel capacity and the achievable data rate that is demanded in many applications such as recording of multichannel neural and retinal prosthesis [19], [20]. Furthermore, in addition to the need of accurate alignment, a further component might be required to be stuck on the patient's skin to overcome the limited communication distance.

In contrast, far-field (FF) WPT offers some practical advantages over NF. By using FF WPT, the link distance between the power supply and the IMD can extend to few meters, which provides more comfort to the patient. Moreover, FF WPT can be utilized in conjunction with other RF energy-harvesting techniques to provide the IMD with a sustainable power flow [21]. The idea behind RF energy-harvesting is that RF signals can concurrently carry energy signals in addition to information signals, which is also known as simultaneous wireless information and power transfer (SWIPT) [22]. The use of SWIPT systems gives IMDs receivers the ability to process information and harvest energy from the same received signal.

Some studies in this field have examined the effect of RF propagation on the biological tissue of the human body, while others were concerned of IMD antenna design [23]–[25]. In fact, there are two common trends in medical implants: deep antenna implants and subdermal antenna implants [26]–[30], [41]. In the former, there is a continued trend of optimization and finding the sweet spot in the trade off for antenna efficiency between reducing the frequency of transmission to increase the penetration versus keeping the

size of the antenna reasonable. For the latter, the trend is towards increasing the frequency while limiting the power of the transmitter below the specific absorption rate (SAR) limit. In our research, we have chosen a frequency band that dictates a subdermal antenna model.

A recent study in [17] has utilized RF for powering wearable devices and demonstrated the electromagnetic compatibility related to WPT systems. In addition, the authors in [31] have deployed the RF energy-harvesting technique to power their prototype of sensor node.

All the aforementioned attempts have only adopted high frequencies of 900 MHz, 2.4 GHz and 5.2 GHz in their studies. However, it is well known that lower frequencies can improve the penetration of electromagnetic (EM) waves into the body which in turn leads to less signal attenuation. Therefore, this paper explores the effect of using medical implant communication service (MICS) band frequencies $(402 - 405 \, \mathrm{MHz})$ on the received energy at the IMD on one hand and its impact on the biological tissues of the human body on the other hand. Furthermore, this paper investigates the feasibility of deploying the WPT system to remotely power the IMD by analyzing the outage probability performance of energy harvested for a FF-powered IMD systems over additive white Gaussian noise (AWGN) channels. Finally, we derive an analytical closed-form expression to explore the effect of access point (AP)-IMD separation on the amount of the harvested energy.

The rest of the paper is organized as follows. The work validation with regards to FCC safety limitation is investigated in Section II, while the details of system and channel model are described in Section III. In Section IV, we derive analytical expressions for the outage probability of the system under consideration. Numerical examples and discussions are presented in Section V. Finally, the paper is concluded in Section VI.

II. VALIDATION OF SAFETY LIMITATION

It is a fact that the power density decreases as $1/r^2$ in free space, however, the main challenge faced by FF powering of IMD is the attenuation caused by the body tissue which impacts negatively on the received signal power at the IMD. Therefore, it is important to understand the capability of receiving power at the IMD that operate at 403 MHz via FF powering. It is worth noting that the Federal Communications Commission (FCC) has determined, for safety purposes, that the maximum permissible exposure (MPE) of power falling on tissue surface, for averaging time of 30 minutes, is $2.7 \, \mathrm{W/m^2}$ at a powering frequency of 403 MHz [32].

As an introduction to this work, we should investigate how much power density should be applied on the tissue surface to continuously power the IMD without exceeding the FCC regulations. A body sensor node (BSN) chip powered by the harvested energy from RF waves and human body heat is assumed in the analysis of this work as a case study to investigate the capability of powering the IMD by FF RF.

A. N. Abdulfattah *et al.*: Performance Analysis of MICS-based RF Wireless Power Transfer System for Implantable Medical Devices

IEEE *Access*

This chip is introduced in [33] and used to wirelessly transmit electrocardiogram (ECG), electromyogram (EMG) and electroencephalogram (EEG) data. The whole chip consumed about 19 μW and was wirelessly powered at 403 MHz. Note that since the MICS is assumed in this work, it is more practical to assume that the chip implant has a subdermal antenna as opposed to deep tissue antenna which is more appropriate for a lower frequency range to enhance the penetration.

Prior to exploring the power density incident on the tissue surface, we should first find the value of power density required at the depth of the implant antenna S_i, which is determined to be 1.194 W/m^2 according to the following formula [34]

$$S_i = \frac{4\pi P_{av}}{e_{mn} e_{rec} G_r \lambda^2},\quad (1)$$

where P_{av} has a value of 19 μW and refers to the average power consumption of the implant, λ represents the operating wavelength below the skin and has a value of 0.14 m at a frequency of 403 MHz [35]. The efficiencies of both matching network e_{mn} and rectification circuit e_{rec} are assumed to be 100 % for the ideal case. Due to the use of low frequency of 403 MHz, a worst case of -20 dB is assumed for the receive antenna gain G_r as it may not be practically possible to utilize the most efficient antenna design because a larger antenna dimension might be required for resonance purposes [24].

Knowing the value of S_i, it is now possible to determine the amount of power density S_1 required to be applied on the tissue surface to continuously power an antenna implanted at a depth $a = 0.01$ m into the body as

$$S_1 = S_i\, e^{\frac{-2a}{\lambda_d}},\quad (2)$$

where λ_d represents the EM skin depth defined as the point at which the EM wave is degraded by a factor of $1/e$ [36]. When the powering frequency f is 403 MHz, λ_d is calculated to be 0.028 m according to the following

$$\lambda_d = \sqrt{\frac{1}{\pi f \mu \sigma}},\quad (3)$$

where μ is the permeability of free space, σ refers to the conductivity of the exposed tissue at 403 MHz and their values are 1.257×10^{-6} m.kg/s^{2}A^2 and 0.8 Sm^{-1}, respectively [37].

The calculation results of (2) and (3) indicate that the required power density at the tissue surface does not exceed the FCC regulations, as S_1 is calculated to be 2.437 W/m^2 which is less than the FCC limit of 2.7 W/m^2.

The ability of the implanted antenna to absorb energy from the power density delivered at the implant can be characterized by the antenna effective area A_e as follows [38]

$$A_e = \frac{P_{av}}{S_i}.\quad (4)$$

Furthermore, it is important to validate that the corresponding antenna size of the implant would be feasible to implement. This can be done using the well known formula for the radius of small loop antenna aperture which is

$$R_{eff} \approx \sqrt{\frac{A_e}{\pi}},\quad (5)$$

where R_{eff} refers to the effective radius of the antenna.

By substituting our previous results in (4) and (5), we get $A_e = 1.6 \times 10^{-5}$ m^2 and accordingly $R \approx 0.23$ cm. This indicate the feasibility of deploying such antennas to capture energy from an external source with a powering frequency of 403 MHz.

The other safety consideration that should be taken into account is that the external source of energy should be located at a safe distance from the human body to avoid exceeding safety limitations. The power density at a specific distance d from the radiating source of energy is given by [34]

$$S(d) = \frac{P_t G_t e_{mn}}{4\pi d^2},\quad (6)$$

where P_t is the transmit power in W and G_t is the isotropic antenna gain in dBi. To find out the minimum allowable source-tissue separation, the MPE limit of power density (2.7 W/m^2) has been substituted in (6) to yield the following relationship

$$d_{min} = \sqrt{\frac{P_t G_t e_{mn}}{10.8\pi}}.\quad (7)$$

In this paper, the values of energy source transmit power and antenna gain are assumed to be 1 W and 0 dBi, respectively, while the matching network efficiency is 100 % as mentioned earlier. Owing to that, the minimum allowable source-tissue separation is calculated to be 17 cm at a powering frequency of 403 MHz.

To conclude, all the analysis that follows in this work can be applied on the IMD as long as the power incident on the tissue surface does not excess 2.7 W/m^2 and the source antenna separation does not go below 17 cm, respectively.
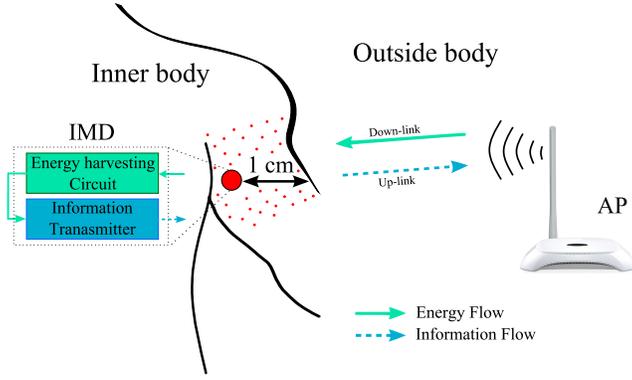
III. SYSTEM AND CHANNEL MODEL

As shown in Fig. 1, we consider an IMD (in-body) with a rechargeable battery and subdermal antenna implanted at a depth of 1 cm into the body and powered wirelessly using off-body AP separated by a distance $d \geq 17$ cm. This AP is dedicated to this application and has one single antenna, transmit power of 1 W, and powering frequency of 403 MHz.

The communication channel between the IMD and the AP can be characterized using the statistical path loss model (in dB) defined by IEEE P802.15, as follows [39]

$$P_L(d) = P_L(d_0) + 10\, n\, log_{10}\left(\frac{d}{d_0}\right) + s\ [\text{dB}],\quad (8)$$

where the shadowing of the signal caused by body parts is represented by the random variable s, which is normally distributed $s \sim \mathcal{N}(0, \sigma^2)$. The reference distance d_0 has been set in this work to be 10 mm and this makes its corresponding path loss $P_L(d_0)$ equal to 57.28 dB, while the path loss

A. N. Abdulfattah *et al.*: Performance Analysis of MICS-based RF Wireless Power Transfer System for Implantable Medical Devices

IEEE *Access*

FIGURE 1. System model illustrating the wireless power transfer during the down-link phase and information transmission during the up-link phase.

exponent n equal to 4.928 [40]. According to that, the down-link channel gain from the AP to the IMD can be presented as follows

$$|h_d|^2 = 10^{-\left(\frac{P_L(d)}{10}\right)} = 10^{-\frac{P_L(d_0)}{10}} \left(\frac{d}{d_0}\right)^{-n} 10^{-\frac{s}{10}}, \quad (9)$$

which can be rewritten as

$$|h_d|^2 = \frac{k}{d^n} 10^{-\frac{s}{10}}, \quad (10)$$

where $k = d_0{}^n 10^{-\frac{P_L(d_0)}{10}}$ and $10^{-\frac{s}{10}} = |h_1|^2$ represents the gain of the shadowing effect that follows a log-normal distribution [41].

Harvest-then-transmit protocol [42], shown in Fig. 2, is deployed in this system where the AP transmits power signal to the IMD during the down-link phase (αT). The IMD can harvest energy from the power signal which is consequently utilized to recharge the battery and then used to transmit the IMD information back to the AP during the up-link phase $(1 - \alpha) T$. In consequence of this, the received signal at the IMD can be expressed as

$$y_i = \sqrt{P_s} h_d x_1 + n_i, \quad (11)$$

where P_s is the AP transmit power, h_d is the AP-to-IMD channel, x_1 is the energy-carrying signal with zero mean and unit power, n_i is the background noise component at the IMD with variance σ_i^2. Now, the harvested energy during αT time is expressed as

$$E_h = \eta \alpha T |y_i|^2 = \eta \alpha T (P_s|h_d|^2 + \sigma_i^2), \quad (12)$$
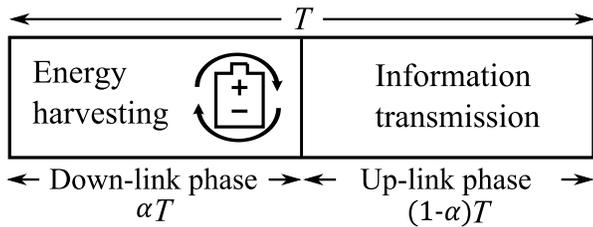
FIGURE 2. Harvest-then-transmit protocol.

where η refers to the energy-harvesting efficiency. By using (10), the harvested energy can be rewritten as

$$E_h = \eta \alpha T \left(\frac{k P_s}{d^n}|h_1|^2 + \sigma_i^2\right). \quad (13)$$

The harvested energy is used in the up-link phase to forward the IMD information to the AP. It is worth mentioning that the energy consumed by the IMD to process the information is commonly negligible compared to the energy used to transmit signal [43]. Hence, the transmitted power at the IMD can be expressed as

$$P_i = \frac{E_h}{(1 - \alpha)T}, \quad (14)$$

and by substituting (13) into (14), we obtain

$$P_i = \frac{\eta \alpha k}{1 - \alpha} \left(\frac{P_s}{d^n}|h_1|^2 + \sigma_i^2\right). \quad (15)$$

Consequently, the received signal at the AP can be defined as

$$y_{ap} = \sqrt{P_i} h_u x_2 + n_{ap}, \quad (16)$$

where h_u is the up-link channel from IMD-to-AP, x_2 denotes the information signal which is normalized as $|x_2|^2 = 1$, and n_{ap}, with variance σ_{ap}^2, refers to the noise at the AP.

Note that when the up-link channel h_u follows the same distribution of down-link channel h_d, then $|h_u|^2 = \frac{k}{d^n} 10^{-\frac{s}{10}}$, where $10^{-\frac{s}{10}}$ represents the shadowing gain $|h_2|^2$ during the up-link phase. By substituting (15) into (16), we can write the signal-to-noise ratio (SNR) at the AP device as follows

$$\gamma_{ap} = \frac{\eta \alpha k^2 \left(\frac{P_s}{d^n}|h_1|^2|h_2|^2 + |h_2|^2\sigma_i^2\right)}{(1 - \alpha)d^n \sigma_{ap}^2}. \quad (17)$$

IV. PERFORMANCE ANALYSIS

In this section, we investigate the performance of the considered system by deriving an analytical expression for the outage probability (P_{out}) of end-to-end communication channel. Also, we provide a closed-form expression for the outage probability of the energy harvested by the IMD. In addition, a closed-form expression is derived for the average harvested energy as a function of the distance between the AP and the IMD.

A. OUTAGE PROBABILITY ANALYSIS

1) SNR OUTAGE PROBABILITY

The outage occurs when the received SNR at the AP, γ_{ap}, falls below a certain threshold γ_{th}, which is given as

$$P_{out} = \Pr\{\gamma_{ap} < \gamma_{th}\}. \quad (18)$$

To simplify our analysis, the γ_{ap} in (17) can be rewritten as

$$\gamma_{ap} = \frac{a|h_1|^2|h_2|^2 + b|h_2|^2}{c}, \quad (19)$$

A. N. Abdulfattah *et al.*: Performance Analysis of MICS-based RF Wireless Power Transfer System for Implantable Medical Devices

IEEE Access

$$P_{out} = Q\left(\frac{\zeta \ln(\frac{b}{\gamma_{th}c}) - 2\mu_1}{2\sigma_1}\right) - \frac{\zeta}{\sqrt{8\pi\sigma_1^2}} \int_{\frac{b}{\gamma_{th}c}}^{\infty} \frac{1}{z} \exp\left(-\frac{(\zeta \ln(z) - 2\mu_1)^2}{8\sigma_1^2}\right) Q\left(\frac{\zeta \ln(\frac{\gamma_{th}cz - b}{a}) - 2\mu_2}{2\sigma_2}\right) dz. \quad (26)$$

where the substitutions a, b, and c are denoted as $\eta\alpha k^2 \frac{P_s}{d^n}$, $\eta\alpha k^2\sigma_i^2$ and $(1-\alpha)\sigma_{ap}^2 d^n$, respectively. Now, by substituting (19) in (18), we obtain

$$P_{out} = \Pr\left\{\frac{a|h_1|^2|h_2|^2 + b|h_2|^2}{c} < \gamma_{th}\right\}, \quad (20)$$

which can also be written, using some algebraic manipulation, as

$$P_{out} = 1 - \Pr\left\{|h_1|^2 > \frac{c\gamma_{th} - b|h_2|^2}{a|h_2|^2}\right\}. \quad (21)$$

According to [43] and [44], the outage probability in (21) can be mathematically calculated as

$$P_{out} = 1 - \int_0^{\frac{b}{\gamma_{th}c}} f_{|h_2|^2}(z)dz - \int_{\frac{b}{\gamma_{th}c}}^{\infty} \bar{F}_{|h_1|^2}\left(\frac{\gamma_{th}cz - b}{a}\right) f_{|h_2|^2}(z)dz, \quad (22)$$

where $f_{|h_2|^2}(.)$ and $\bar{F}_{|h_1|^2}(.)$ are the probability distribution function (pdf) and the complementary commutative distribution function (ccdf) of the channel gains $|h_2|^2$ and $|h_1|^2$, respectively. As previously stated in Section III that both $|h_1|^2$ and $|h_2|^2$ are log-normally distributed, we can express $f_{|h_2|^2}(.)$ and $\bar{F}_{|h_1|^2}(.)$, respectively, as follows [45]

$$f_{|h_2|^2}(z) = \frac{\zeta}{z\sqrt{8\pi\sigma_1^2}} \exp\left(-\frac{(\zeta \ln(z) - 2\mu_1)^2}{8\sigma_1^2}\right), \quad (23)$$

and

$$\bar{F}_{|h_1|^2}\left(\frac{\gamma_{th}cz - b}{a}\right) = Q\left(\frac{\zeta \ln(\frac{\gamma_{th}cz - b}{a}) - 2\mu_2}{2\sigma_2}\right), \quad (24)$$

where $\zeta = \frac{10}{\ln(10)}$ and $Q(.)$ is the Q-function defined as

$$Q(x) = \frac{1}{2} - \frac{1}{2}\text{erf}\left(\frac{x}{\sqrt{2}}\right), \quad (25)$$

where $\text{erf}(.)$ is the error function. Finally, by substituting (23) and (24) into (22), we can express the system outage probability as in (26), which is shown at the top of the next page.

2) OUTAGE PROBABILITY OF ENERGY-HARVESTING

To assess the feasibility of employing the WPT system for our proposed scenario, a closed-form expression is derived for the outage probability of energy-harvesting for the down-link channel, where the energy is transferred from the AP to the IMD. The outage for a given value of energy-harvesting can be expressed as

$$P_{out} = \Pr\{E_h < \bar{E}_h\}, \quad (27)$$

where $\bar{E}_h$ refers to the threshold value of energy-harvesting. Now, using (13), the P_{out} can be expressed as

$$P_{out} = \Pr\left\{\frac{\eta\alpha TkP_s}{d^n}|h_1|^2 + \sigma_i^2 < \bar{E}_h\right\},$$
$$= \Pr\left\{|h_1|^2 < \frac{(\bar{E}_h - \sigma_i^2)d^n}{\eta\alpha TkP_s}\right\}. \quad (28)$$

Since $|h_1|^2$ is log-normally distributed, the P_{out} in (28) can be denoted as the cdf of the log-normal distribution mentioned in (23). Therefore, the final result of P_{out} can be written as

$$P_{out} = \frac{1}{2}[\text{erf}(v) + 1], \text{ where } v = \frac{\zeta \ln\left(\frac{(\bar{E}_h - \sigma_i^2)d^n}{\eta\alpha TkP_s}\right) - 2\mu_1}{\sqrt{8}\sigma_1}. \quad (29)$$

It is worth mentioning that when the outage happens in one block during the down-link phase, the energy harvested E_h within this block will be 0. As the system is digital, it will behave in go/no go mode. Re-arranging equation (14), we find out that $E_h = P_i(1 - \alpha)T$. This will dictate that α will be set to 1 in order for this equation to stay satisfied which in turn means that the value of α for the next block becomes 1 or in other words the system enters a no-transmission phase and goes into full down-link mode waiting for the harvested energy to exceed the threshold. The loss of the up-link in the system can be used as a trigger for the transmitter to increase its power to the maximum permissible, to give an alert for shadowing effect or to give an alert for a loss of signal. During the outage over an extended period of time, the implant will use the previously harvested energy stored in some capacitor or inner battery. However, when the outage continues for several time blocks, the system enters in an idle state to save the battery until a wakeup signal is received again.

B. EFFECT OF DISTANCE ON THE ENERGY-HARVESTING

Knowing the minimum allowable distance between the AP and IMD, it is necessary to investigate the maximum distance that the AP can be placed away from the IMD, while ensuring that the IMD can still harvest energy from the AP. Therefore, in this section, we derive a closed-form expression to investigate the effect of AP-IMD separation on the amount of the harvested energy.

A. N. Abdulfattah *et al.*: Performance Analysis of MICS-based RF Wireless Power Transfer System for Implantable Medical Devices

IEEE *Access*

The random variable y which represents the instantaneous channel gain in decibel is directly proportional to the log-normal distribution as

$$\ln(y) \propto \ln(z), \tag{30}$$

where z is a normal random variable and $\ln(z)$ is a log-normal random variable.

By assuming that the power is normalized, and with some algebraic manipulations, the linear value of the channel gain can be written as

$$\ln(y) = \frac{1}{\zeta}\ln(z), \tag{31}$$

where $\frac{1}{\zeta} = \frac{\ln(10)}{10}$ is the proportional constant. Then, by using the properties of logarithmic functions, we have

$$y = z^{\frac{1}{\zeta}}. \tag{32}$$

It is well known that the probability does not change by transforming the variables, since the probability is the area under the curve, then

$$\int g(z)dz = \int f(y)dy, \tag{33}$$

which means that $g(z)dz = f(y)dy$. Accordingly, $f(y)$ can be written as

$$f(y) = g(z)\frac{dz}{dy}\Big|_{z=y}, \tag{34}$$

where $g(z) = \frac{1}{\sqrt{2\pi}z\sigma}\exp\big(-\frac{(\ln(z)-\mu)^2}{2\sigma^2}\big)$ [46].

Using (32) with some algebraic manipulation, the pdf of the log-normal distribution $f(y)$ can now be expressed as

$$f(y) = \frac{\zeta}{\sqrt{8\pi}y\sigma'}\exp\left(-\frac{(\zeta\ln(y)-2\mu')^2}{8\sigma'^2}\right), \tag{35}$$

where $\mu' = 0.5\mu$, $\sigma' = 0.5\sigma$, and $0 < y < \infty$.

As the channel from AP-to-IMD is log-normally distributed, the pdf in (35) is used to model the distribution of $|h_1|^2$. The mean value of this distribution can be found by $\mathbb{E}[f(y)]$ which equals to $\mathbb{E}[z^{\frac{1}{\zeta}}]$ in the usual log-normal distribution.

Using (13), the instantaneous harvested energy at the IMD for zero-mean noise can be expressed as

$$E_h = \frac{\eta\alpha TkP_s}{d^n}|h_1|^2. \tag{36}$$

To obtain the average value of the harvested energy, we use

$$\mathbb{E}[E_h] = a\mathbb{E}[|h_1|^2], \tag{37}$$

$$= a\int_0^\infty yf(y)dy, \tag{38}$$

where $a = \frac{\eta\alpha TkP_s}{d^n}$. Substituting (32) into (38), we can express the expectation of the energy-harvesting as

$$\mathbb{E}[E_h] = a\int_0^\infty \frac{z^{\frac{1}{\zeta}-1}}{\sqrt{2\pi}\sigma}\exp\left(-\frac{(\ln(z)-\mu)^2}{2\sigma^2}\right)dz. \tag{39}$$

Using change of variable method, let $z = e^{-x}$ and $dz = -e^{-x}dx$. Substituting z and dz in (39), we obtain

$$\mathbb{E}[E_h] = a\int_{-\infty}^\infty \frac{e^{-\frac{x}{\zeta}}}{\sqrt{2\pi}\sigma}\exp\left(-\frac{(x+\mu)^2}{2\sigma^2}\right)dx. \tag{40}$$

Now, using some algebraic manipulations, we can rewrite (40) as

$$\mathbb{E}[E_h] = a\exp\left(\frac{2\mu\zeta+\sigma^2}{2\zeta^2}\right) \times$$
$$\int_{-\infty}^\infty \frac{1}{\sqrt{2\pi}\sigma}\exp\left(-\frac{\left(x+(\mu+\frac{\sigma^2}{\zeta})\right)^2}{2\sigma^2}\right)dx. \tag{41}$$

The integration is the whole area under the curve of the pdf of the Gaussian random variable which is by definition equals to 1. That is since $\int_{-\infty}^\infty \frac{1}{\sqrt{2\pi}\sigma}\exp\big(-\frac{(x-\mu)^2}{2\sigma^2}\big)dx = 1$ for any σ or μ. With this in mind, and by substituting μ' and σ' in (41), the average value of the harvested energy can be denoted as

$$\mathbb{E}[E_h] = a\exp\left(\frac{2(\mu'\zeta+\sigma'^2)}{\zeta^2}\right). \tag{42}$$

V. NUMERICAL RESULTS AND DISCUSSION

In this section, some numerical examples and Monte Carlo-based simulations are presented to asses the validity of the closed-form expressions derived above. It can be clearly seen that there is strong agreement between the simulations and theoretical results in all figures, which verifies the accuracy of our analysis. Throughout this section, it is considered that the IMD is embedded in the left hand below the skin at a depth of $d_0 = 10$ mm. In addition, we use $\eta = 1$ for simplicity.

Based on (26), the end-to-end communication system performance is examined and depicted in Fig. 3 where the two main factors: the SNR threshold and the distance d between IMD-AP are considered to illustrate their impact on the system outage probability. The simulation results indicate that as the threshold value increases, the outage probability increases, for different values of the separation distance d. In addition, it is also observed that when the AP is located at the minimum allowable distance ($d = 0.17$ m), the outage probability is almost zero for all different values of SNR threshold. Following the increase of distance to 0.5 m, an acceptable increase in the outage probability is recorded. However, the system performance experiences unacceptable large values of outage probability when the AP placed 1 m away from the human body. On this basis, it is preferable not to exceed a distance of half a meter to ensure reliable communication.
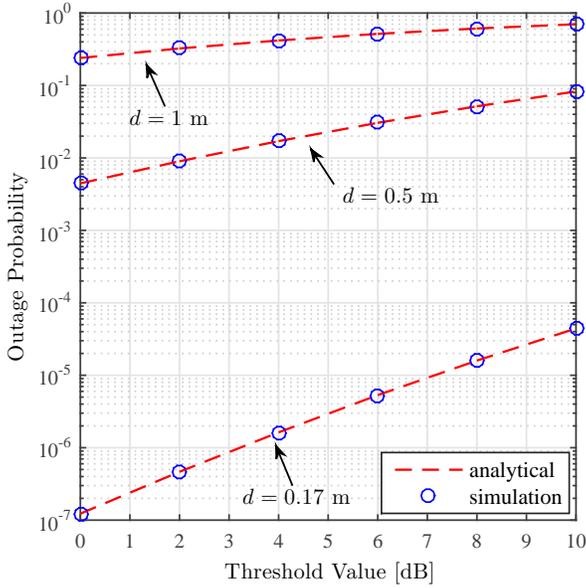
A. N. Abdulfattah *et al.*: Performance Analysis of MICS-based RF Wireless Power Transfer System for Implantable Medical Devices

IEEE *Access*

FIGURE 3. Outage probability performance versus SNR threshold for different values of distance d.
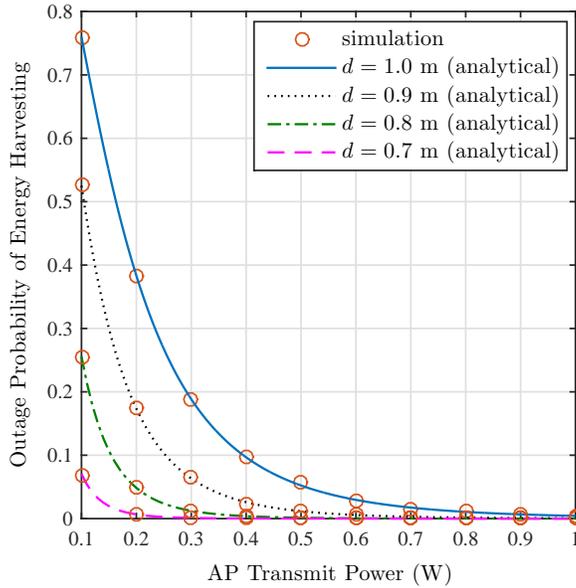

FIGURE 4. Effect of AP transmit power on the outage probability of energy-harvesting.

It is important to guarantee a continuous charging without interruptions during the energy-harvesting time. Therefore, an essential requirement for successful operation of IMD is the existence of adequate transmit power. Owing to that, the effect of the source transmit power on the outage probability of energy-harvesting is investigated, using the derived formula in (29), and illustrated in Fig. 4, where the threshold value of energy harvesting and minimum allowable value of outage probability are assumed to be $\bar{E}_h = 0.5$ mJ and
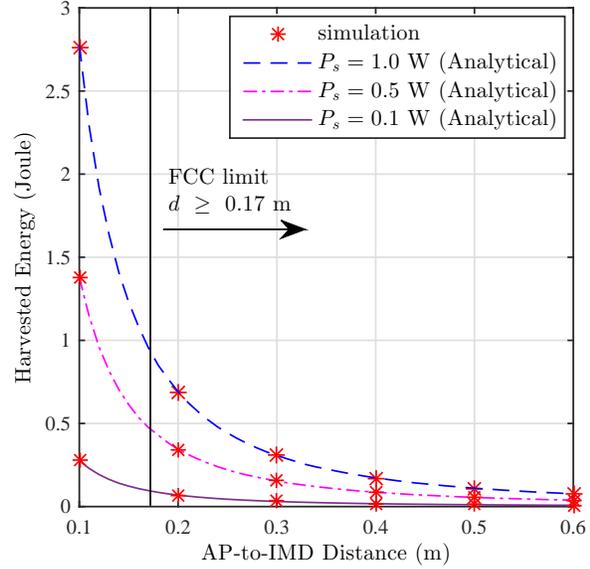

FIGURE 5. Effect of distance on the amount of the harvested energy.

$P_{out} < 0.1$, respectively. It can be concluded from Fig. 4, when the AP is placed 1 m away from the body surface, it is not feasible to use a source transmit power of less than 0.5 W due to the high possibility of outage occurrence, whereas the probability of outage is approaching zero at higher transmit power, specifically more than 0.5 W.

To comply with the FCC limitation and to ensure continuous and reliable operation of energy-harvesting without any interruption, we suggest to shorten the distance between the AP and the IMD to less than 1 m. This also accords with our findings in Fig. 5, which shows that decreasing the distance between the AP and the body surface results in more harvested energy at the IMD, which in turn, lowers the outage probability. It is worth mentioning that our findings shown in both Fig. 4 and Fig. 5 are based on energy-harvesting time of $\alpha = 0.5$, while the derived formula in (42) is used to find the average harvested energy depicted in Fig. 5.

According to (42), the amount of harvested energy can be greatly affected by the time slot allocated for energy-harvesting process during the down-link phase. Therefore, we have studied the variation effect of energy-harvesting time, α, on the amount of the harvested energy where three different values of distances are considered. The results depicted in Fig. 6 show that as the energy-harvesting time increases, the amount of harvested energy increases, irrespective of the separation distance values. However, the greatest value of energy-harvesting is occurred when the AP is placed away from the body at the minimum allowable distance $d = 0.17$ m. On the other hand, as the harvest-then-transmit protocol is employed, the increase in harvest time is offset by a decrease in the time of data transmission during the up-link phase and vice versa.

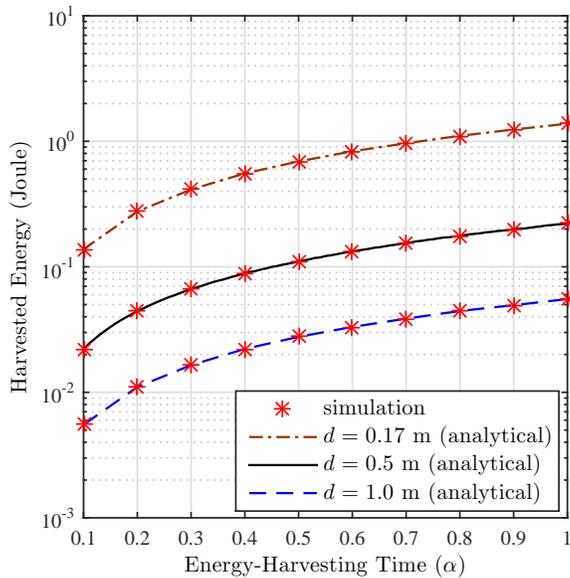The outage probability as a function of energy-harvesting

FIGURE 6. Effect of energy harvesting time on the amount of the harvested energy.

FIGURE 7. Outage probability performance as a function of energy harvesting time and threshold value.

time and threshold value is shown in Fig. 7, where $n = 4.22$, $P_s = 1$ W, and $d = 1$ m. It can be easily observed that increasing the threshold value leads to an increase in the probability of interrupting the energy-harvesting operation regardless of the time α allocated for energy-harvesting. In addition, the results show that the performance improves as the energy-harvesting time increased irrespective of the energy-harvesting threshold value. This is due to the fact that increasing the harvesting time means more energy to be harvested. It is also noticeable that when the threshold is very large, the outage probability becomes very high and approaching 1 for all different values of energy-harvesting time.

VI. CONCLUSION

The main purpose of our work was to provide the implantable medical devices with a perpetual energy source. Accordingly, the feasibility of deploying far-field RF powering in combined with energy-harvesting technique was investigated. An access point with a powering frequency of 403 MHz and transmit power of 1 W was used for wireless power transfer. Harvest-then-transmit protocol was considered in our proposed system, where the access point transmits power signal to the implanted device during the down-link phase. The power signal is consequently be used to recharge the battery and transmit the implants information back to the access point during the up-link phase. Our results showed that in order to maintain an outage probability of less than 10^{-1}, a minimum source transmit power of 0.4 W was required, considering that the threshold value of energy-harvesting and AP-IMD separation are 0.5 mJ and 1 m, respectively. It is also presented that the minimum allowable
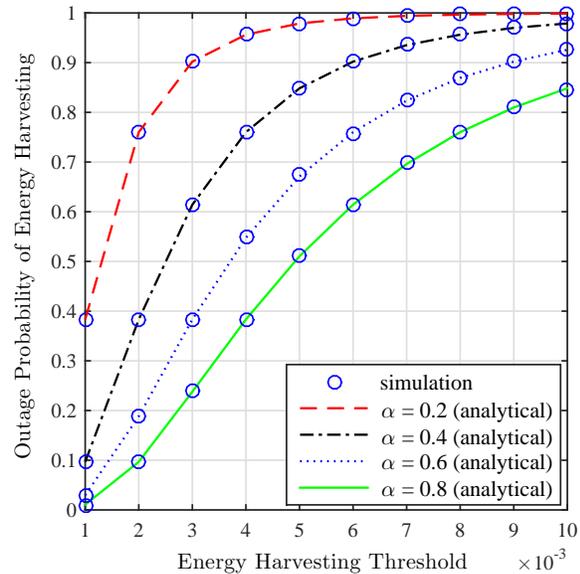
distance between the AP and the body surface was 17 cm at a powering frequency of 403 MHz, while the system performance experienced high outage probability when the distance was beyond 0.5 m.

REFERENCES

[1] J. Hsieh, Y. Huang, P. Kuo, T. Wang and S. Lu, "A 0.45-V Low-Power OOK/FSK RF Receiver in 0.18 μm CMOS Technology for Implantable Medical Applications," *IEEE Trans. Circuits Syst. I, Reg. Papers*, vol. 63, no. 8, pp. 1123-1130, Aug. 2016.

[2] Abdulfattah, A. N., C. C. Tsimenidis, and A. Yakovlev. "Ultra-Low Power m-Sequence Code Generator for Body Sensor Node Applications." *Integration, the VLSI Journal, Elsevier*, 2017.

[3] E. Katz, "Implantable Biofuel Cells Operating In Vivo Potential Power Sources for Bioelectronic Devices," *Bioelectron. Medicine*, vol. 2, no. 1, pp. 1-12, Jun. 2015.

[4] E. Katz, "Implantable Biofuel Cells Operating in vivo: Providing Sustainable Power for Bioelectronic Devices: From Biofuel Cells to Cyborgs," 6th *Int. Workshop on Advances in Sensors and Interfaces (IWASI)*, 2015, pp. 2-13.

[5] J. Katic and S. Rodriguez and A. Rusu, "A High-Efficiency Energy Harvesting Interface for Implanted Biofuel Cell and Thermal Harvesters," *IEEE Trans. Power Electron.*, vol. 33, no. 5, pp. 4125-4134, May 2018.

[6] Fan, Kangqi and Liu, Zhaohui and Liu, Haiyan and Wang, Liansong and Zhu, Yingmin and Yu, Bo, "Scavenging Energy from Human Walking Through a Shoe-mounted Piezoelectric Harvester," *Appl. Physics Lett.*, vol. 110, no. 14, pp. 143902, 2017.

[7] J. Cao, "Optimization of TEG for Human Body Powered Mobile Devices," 17th *IEEE Intersociety Conf. on Thermal and Thermomechanical Phenomena in Electron. Syst. (ITherm).*, 2018, pp. 1000-1008.

[8] Z. M. Dalala, "Energy Harvesting Using Thermoelectric Generators," *IEEE Int. Energy Conf. (ENERGYCON).*, 2016, pp. 1-6.

[9] Q. Wan and Y. Teh and Y. Gao and P. K. T. Mok, "A Analysis and Design of a Thermoelectric Energy Harvesting System With Reconfigurable Array of Thermoelectric Generators for IoT Applications," *IEEE Trans. Circuits Syst. I, Reg. Papers.*, vol. 64, no. 9, pp. 2346-2358, Sept. 2017.

[10] Cadei, Andrea and Dionisi, Alessandro and Sardini, Emilio and Serpelloni, Mauro, "Kinetic and Thermal Energy Harvesters for Implantable Medical Devices and Biomedical Autonomous Sensors," *Measurement Sci. and Technology.*, vol. 25, no. 1, pp. 012003, 2013.

[11] T. Wu, J. RedoutÃľ and M. R. Yuce, "A Wireless Implantable Sensor Design With Subcutaneous Energy Harvesting for Long-Term IoT Healthcare Applications," *IEEE Access*, vol. 6, pp. 35801-35808, 2018.

[12] Song, Kwangsun and Han, Jung Hyun and Lim, Taehoon and Kim, Namyun and Shin, Sungho and Kim, Juho and Choo, Hyuck and Jeong, Sungho and Kim, Yong-Chul and Wang, Zhong Lin, "Subdermal Flexible Solar Cell Arrays for Powering Medical Electronic Implants," *Advanced healthcare materials*, vol. 5, no. 13, pp. 1572-1580, March. 2016.

[13] S. Kim and R. Vyas and J. Bito and K. Niotaki and A. Collado and A. Georgiadis and M. M. Tentzeris,"Ambient RF Energy-Harvesting Technologies for Self-Sustainable Standalone Wireless Sensor Platforms," *Proc. IEEE*, vol. 102, no. 11, pp. 1649-1666, Nov. 2014.

[14] P. Li and R. Bashirullah, "A Wireless Power Interface for Rechargeable Battery Operated Medical Implants," *IEEE Trans. Circuits Syst. II*, vol. 54, no. 10, pp. 912-916, Oct. 2007.

[15] A. K. RamRakhyani, S. Mirabbasi and M. Chiao, "Design and Optimization of Resonance-Based Efficient Wireless Power Delivery Systems for Biomedical Implants," *IEEE Trans. Biomed. Circuits Syst.*, vol. 5, no. 1, pp. 48-63, Feb. 2011.

[16] T. Campi, S. Cruciani, M. Feliziani and A. Hirata, "Wireless Power Transfer System Applied to an Active Implantable Medical Device," *IEEE Wireless Power Transfer Conf.*, 2014, pp. 134-137.

[17] G. Monti et al., "EMC and EMI Issues of WPT Systems for Wearable and Implantable Devices," *IEEE Electromagn. Compat.*, vol. 7, no. 1, pp. 67-77, First Quarter 2018.

[18] R. Xue and K. Cheng and M. Je, "High-Efficiency Wireless Power Transfer for Biomedical Implants by Optimal Resonant Load Transformation," *IEEE Trans. Circuits Syst. I, Reg. Papers*,vol. 60, no. 4, pp. 867-874, Apr. 2013.

[19] R. Bashirullah, "Wireless Implants," *IEEE Microw. Mag.*,vol. 11, no. 7, pp. S14-S23, Dec. 2010.

[20] A. M. Sodagar and K. D. Wise and K. Najafi, "A Wireless Implantable Microsystem for Multichannel Neural Recording," *IEEE Trans. Microw. Theory Tech.*,vol. 57, no. 10, pp. 2565-2573, Oct. 2009.

[21] X. Lu, P. Wang, D. Niyato, D. I. Kim and Z. Han, "Wireless Networks With RF Energy Harvesting: A Contemporary Survey," *IEEE Commun. Surveys Tuts.*, vol. 17, no. 2, pp. 757-789, Second quarter 2015.

[22] D. Sui, F. Hu, W. Zhou, M. Shao and M. Chen, "Relay Selection for Radio Frequency Energy-Harvesting Wireless Body Area Network With Buffer," *IEEE Internet Things J.*, vol. 5, no. 2, pp. 1100-1107, Apr. 2018.

[23] Chow, E.Y., Yang, C. and Irazoqui, "Wireless Powering and Propagation of Radio Frequencies Through Tissue", in *Wireless Power Transfer*. Denmark: River Publisher, 2012, pp. 303-331.

[24] R. A. Bercich, D. R. Duffy and P. P. Irazoqui, "Far-Field RF Powering of Implantable Devices: Safety Considerations," *IEEE Trans. Biomed. Eng.*, vol. 60, no. 8, pp. 2107-2112, Aug. 2013.

[25] A. Mouapi and N. Hakem, "Performance Evaluation of Wireless Sensor Node Powered by RF Energy Harvesting," *16th Mediterranean Microwave Symp. (MMS)*, Abu Dhabi, 2016, pp. 1-4.

[26] O. H. Murphy and C. N. McLeod and M. Navaratnarajah and M. Yacoub and C. Toumazou, "A Pseudo-Normal-Mode Helical Antenna for Use With Deeply Implanted Wireless Sensors," *IEEE Trans. Antennas Propag.*, vol. 60, no. 2, pp. 1135-1139, Feb. 2012.

[27] A. K. Skrivervik, "Implantable Antennas: The challenge of Efficiency," *2013 7th European Conf. on Antennas and Propag. (EuCAP)*, 2013, pp. 3627-3631.

[28] W. Xia and K. Saito and M. Takahashi and K. Ito, "Performances of an Implanted Cavity Slot Antenna Embedded in the Human Arm," *IEEE Trans. Antennas Propag.*, vol. 57, no. 4, pp. 894-899, Apr. 2009.

[29] E. G. Kilinc and M. A. Ghanad and F. Maloberti and C. Dehollain, "A Remotely Powered Implantable Biomedical System With Location Detector," *IEEE Trans. Biomed. Circuits Syst.*, vol. 9, no. 1, pp. 113-123, Feb. 2015.

[30] Monti, Giuseppina and De Paolis, Maria Valeria and Corchia, Laura and Mongiardo, Mauro and Tarricone, Luciano, "Inductive Link for Power and Data Transfer to a Medical Implant," *Wireless Power Transfer*, vol. 4, no. 2, pp. 98-112, 2017.

[31] H. Nishimoto, Y. Kawahara and T. Asami, "Prototype Implementation of Ambient RF Energy Harvesting Wireless Sensor Networks," *Proc. of IEEE Sensors*, 2010, pp. 1282-1287.

[32] D. L. Means, K. W. Chan. "Evaluating Compliance with FCC Guidelines for Human Exposure to Radio Frequency Electromagnetic Fields". *OET bulletin, 65*, Washington, D.C., USA, 1997, PP. 25-26.

[33] Y. Zhang et al., "A Batteryless 19 μW MICS/ISM-Band Energy Harvesting Body Sensor Node SoC for ExG Applications," *IEEE J. Solid-State Circuits*, vol. 48, no. 1, pp. 199-213, Jan. 2013.

[34] Pozar, D.M., " *Microwave and RF design of wireless systems*", New York: Wiley, 2001, pp. 81-97.

[35] Conor P, "Antenna Designs for Wireless Medical Implants", Master dissertation. *Antenna and High Frequency Research Centre, Dublin Institute of Technology*, 2013, doi:10.21427/D7P60G.

[36] Seybold, J.S., "*Introduction to RF propagation*". Canada: John Wiley & Sons, 2005, pp. 14-66.

[37] Gabriel, C., "Compilation of the Dielectric Properties of Body Tissues at RF and Microwave Frequencies", *King's coll. London Dept. of physics*, UK, Jan. 1996.

[38] Ulaby, F.T., Michielssen, E. and Ravaioli, U., "*Fundamentals of Applied Electromagnetics* ", 6th ed. USA: Prentice Hall, 2001, pp. 404-444.

[39] IEEE Working Group for Wireless Personal Area Networks (WPANs), *IEEE Standard P802.15*, 2009.

[40] Yangzhe Liao, M. S. Leeson and M. D. Higgins, "An In-body Communication Link Based on 400 MHz MICS Band Wireless Body Area Networks," *IEEE 20th Int. Workshop on Comput. Aided Modeling and Design of Commun. Links and Networks (CAMAD)*, Guildford, 2015, pp. 152-155.

[41] G. D. Ntouni, A. S. Lioumpas and K. S. Nikita, "Reliable and Energy-Efficient Communications for Wireless Biomedical Implant Systems," *IEEE J. Biomed. Health Inform.*, vol. 18, no. 6, pp. 1848-1856, Nov. 2014.

[42] H. Ju and R. Zhang, "Throughput Maximization in Wireless Powered Communication Networks," *IEEE Trans. Wireless Commun.*, vol. 13, no. 1, pp. 418-428, January 2014.

[43] K. M. Rabie, B. Adebisi and M. Rozman, "Outage Probability Analysis of WPT Systems with Multiple-Antenna Access Point," *10th Int. Sym. on Commun. Syst., Networks and Digital Signal Process. (CSNDSP)*, Prague, 2016, pp. 1-5.

[44] A. A. Nasir and X. Zhou and S. Durrani and R. A. Kennedy, "Relaying Protocols for Wireless Energy Harvesting and Information Processing," *IEEE Trans. Wireless Commun.*, vol. 12, no. 7, pp. 3622-3636, July 2013.

[45] K. M. Rabie and B. Adebisi and M. Alouini, "Wireless Power Transfer in Cooperative DF Relaying Networks with Log-Normal Fading," *2016 IEEE Global Commun. Conf. (GLOBECOM)*, 2016, pp. 1-6.

[46] J.G. Proakis and M. Salehi, *Digital Communications*, 5th ed, McGraw-Hill, New York, NC, 2008, pp. 54-55.